

## **Study of A Ferroelectric Liquid Crystal Mesogen by Geometrical Optimization and Electro-Optic Characterization**

**D. Goswami\***

Department of Physics, St. Joseph's College, Darjeeling 734104, India

Received 30 March 2023, accepted in final revised form 1 November 2023

### **Abstract**

In the present work one biphenyl benzoate cored liquid crystal was characterized using geometrical optimization and electro-optic study. Geometry of the molecule was optimized using Hartree-Fock method with 3-21G basis. The simulated value of molecular length and dipole moment was reported. The Infrared (IR) spectra were also simulated and analyzed. The energy gap between highest occupied molecular orbit (HOMO) and lowest unoccupied molecular orbit (LUMO) was calculated. The phase transition temperatures and phase sequences were identified by observing the topological defects in the optical textures at different temperatures under polarizing microscope. It exhibited ferroelectric smectics C\* (SmC\*) phase for a wide range of temperature and then directly melted into isotropic phase. The optical tilt angle of the compound was measured in SmC\* phase and was fitted with mean field model to explore the nature of phase transition. The applicability of the compound for display applications were judged based on the parameters measured.

*Keywords:* Ferroelectric liquid crystal; Hartree-Fock formalism; Polarizing optical microscopy; Optical tilt.

© 2024 J.S.R. Publications. ISSN: 2070-0237 (Print); 2070-0245 (Online). All rights reserved.  
doi: <http://dx.doi.org/10.3329/jsr.v16i1.65364> J. Sci. Res. **16** (1), 97-105 (2024)

### **1. Introduction**

Liquid crystals have remained to be in the focus of research interest for last few decades for their unique properties which combines the characteristics of both conventional liquid (like fluidity) and that of crystal (like dielectric anisotropy). Due to these hybrid properties of liquid crystals, these had extensively been used to produce display devices. In fact currently liquid crystal displays (LCDs) have almost completely replaced its earlier counter parts like cathode ray tubes (CRTs) in the market. However, most of these LCDs are based on nematic liquid crystals, which have slower electric response time and smaller viewing angle. Ferro electric liquid crystals (FLCs), which have permanent electric dipole moments show much faster electric response (in microsecond range) compared to nematics, thus they have emerged as promising material for fast electro-optic applications[1-4]. Yet, ferroelectric liquid crystal displays are still not much used commercially for difficulties in different levels like less thermal stability of ferroelectric

---

\*Corresponding author: [sangdin@gmail.com](mailto:sangdin@gmail.com)

phases (like SmC\* phase), high rotational viscosity etc. Liquid crystals with biphenyl core usually show high thermal, chemical stability and low rotational viscosity [5]. Introduction of a third benzene ring linked with the biphenyl core with an ester group results a biphenyl benzoate core. Liquid crystal with such core, usually show wide range low temperature ferroelectric and antiferroelectric phases [6-8]. Due to the angle of ester group, biphenyl benzoate cored liquid crystals usually exhibit highly tilted ferroelectric or antiferroelectric liquid crystals. Keeping these in mind, one biphenyl benzoate based chiral liquid crystal namely (S)-(+)-4-[(3-undecafluoro-hexanoyloxy)prop-1-oxy]biphenyl-4-yl 4-(1-methylheptyloxy)-benzoate (Code name: 5F3R) [6,9] is selected for investigation. This compound have a biphenyl benzoate core and displays only SmC\* phase (ferroelectric phase) for a broad temperature range. The molecular structure of the compound and its phase sequence is shown in Fig. 1. To explore the structural-property relationship the molecular structure of 5F3R was optimized. A few optimized parameters (molecular length and dipole moment) of the compound were published before using parametric3 (PM3) method method [9]. In this paper more detailed optimized properties (molecular length, dipole moment, IR spectra, HOMO-LUMO gap, ionization potential, electron affinity etc.) of the molecule will be reported using Hartree-Fock formalism, which is more reliable than PM3. The optical tilt angle of 5F3R will also be reported here for the first time which is a critical parameter of FLCs from the perspective of display applications. The optical textures of 5F3R in different phases, which is an important tool to explore the topological defects of the compound in the said phases, will also be discussed.

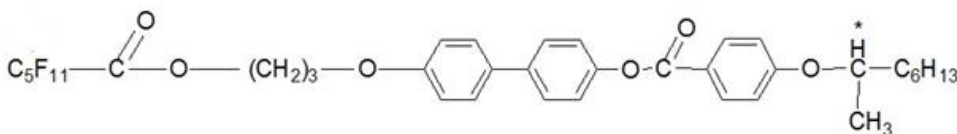


Fig. 1. Molecular structure of 5F3R. Phase transition temperatures: Crystal (75 °C) 83 °C SmC\* 139.5 °C isotropic [6,9].

## 2. Experimental Methods

Using optical polarizing microscopy the transition temperatures of the compound were measured and phases were identified. An Olympus BX41 polarizing microscope (magnification 20X) equipped with a CCD camera (With resolution of 2592 X 1944 dpi) was used for this purpose. The liquid crystal sample was fed into a commercially available EHC liquid crystal cell of 5  $\mu\text{m}$  thickness with low resistivity (about 20  $\Omega/\text{cm}^2$ ) and with transparent indium tin oxide (ITO) electrodes by capillary action in isotropic state. Homogeneous alignment of the sample was ensured by the polymer layer coated inside the glass wall of the cell. Same cell was used to measure the optical tilt angle ( $\theta$ ) of the compound in SmC\* phase. The sample inside the cell was electrically switched under a low frequency (10 Hz and 10 V) square wave and was simultaneously observed under

polarizing microscope. Under the application of the field, liquid crystal molecules in bistable ferroelectric SmC\* phase may rotate around an imaginary cone by twice the tilt angle. Initially the sample stage was rotated to a position of minimum transmission under cross polarizer. When the field was reversed the molecules of the FLC tilted in opposite direction. FLCs being optically active materials, it rotated the polarized light along its own axis and the transmission didn't remain minimum anymore. To achieve the dark state once again, the sample stage had to be rotated by a certain angle. The angle of rotation of the sample between two consecutive dark states gave us a direct measure of  $2\theta$ . The geometry of the molecular rotation is in Fig. 2. The details of the procedure is mentioned elsewhere [10]. For all these experiments the temperature was controlled with an accuracy of  $\pm 0.1$  °C using a FP82HT hotstage and a Mettler FP90 temperature controller.

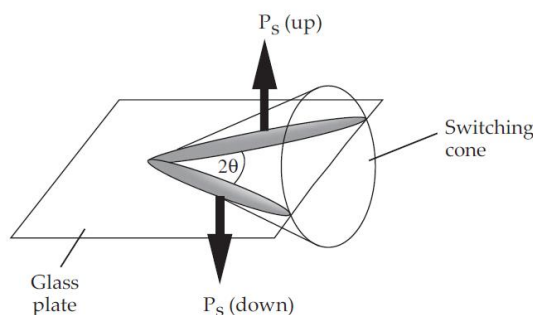


Fig. 2. Bistable rotation of molecule in SmC\* phase [11].

### 3. Results and Discussion

#### 3.1. Optimized molecular geometry

The molecular geometry plays a key role in the molecular interactions of the mesogenic compounds affecting many of its bulk properties. To inculcate this effect the molecular structure of 5F3R was optimized. In a previous paper the optimized length and dipole moment of 5F3R was reported using PM3 molecular mechanics method [9]. But PM3 method is a semi-empirical quantum method which is an approximation of Hartree-Fock formalism and it obtains some parameters from empirical data. Hartree-Fock is an ab initio method used to calculate the electronic structure and energy of a molecule by solving many body time independent Schrodinger's equation. To include the effect of Pauli's exclusion principle the wave function is constructed with help of a Slater determinant. To solve the equation the method starts from an initial guess of electron distribution and refines it iteratively until it converges to a self consistent value. After achieving the self consistent electron distribution the energy of the electrons and the molecule are measured. Though PM3 is numerically less expensive than Hartree-Fock method but is also less accurate for our molecule [12]. Keeping that in mind we have

optimized the geometry again applying Hartree-Fock method using 3-21G basis set in a commercial package [13]. The optimized structure is shown in Fig. 3.

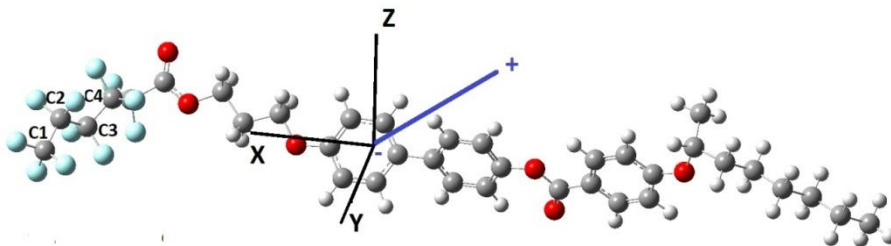


Fig. 3. Optimized geometry of 5F3R.

The optimized length of 5F3R was 35.19Å. This is longer than the optimized length of two other compounds of same series namely 2F3R and 3F3R [14]. It was expected as 2F3R and 3F3R have shorter fluorinated chain compared to 5F3R. The dipole moment ( $\mu$ ) of 5F3R was 6.53D (-5.05, 0.39, 4.12), where the components of dipole moments along three axis are shown in bracket. The fluorine chain plays an important role on the dipole moment of the molecule. To explore the conformation of the fluorine chain we have measured the torsion angle among the atoms C1, C2, C3 and C4 which was found to be -156.95°.

The IR spectrum of this molecule was also calculated using the same package. The simulated IR spectrum of isolated 5F3R molecule (variation of molar extinction coefficient ( $\epsilon$ ) with frequency) is shown in Fig. 4.

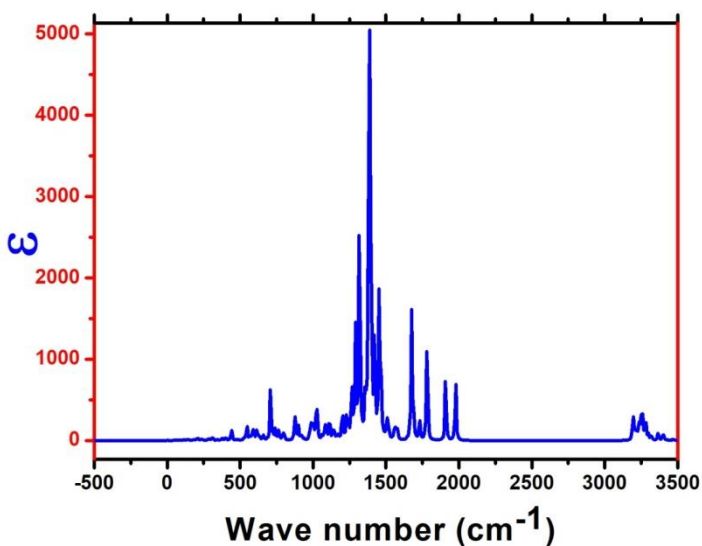


Fig. 4. Simulated IR spectra of 5F3R.

For the complexity of simulated vibrational modes it was not possible to assign each band. However, from the typical values of different vibrational frequencies of different bond and observing the vibrations of the simulated molecule at different frequencies in Gauss view software, we have tried to analyze few specific dominating vibrations [15]. The highest peaks at around  $1390\text{-}1400\text{ cm}^{-1}$  are for the breathing of the phenyl rings in the core and C-F stretching in the fluorinated chain of the molecule. The absorptions near about  $3200\text{ cm}^{-1}$  can be assigned with the C-H stretching in the protonated chain. Peaks near  $700\text{ cm}^{-1}$  are due to C-F wagging in the fluorinated chain.

According to frontier orbital theory the knowledge of the highest occupied molecular orbit (HOMO) and lowest unoccupied molecular orbit (LUMO) is important to understand the reactions involving  $\pi$  orbital of  $\pi$  conjugated system [12,16]. Fig. 5 shows the simulated HOMO (5a) and LUMO (5b) surfaces of the molecule 5F3R. As can be observed both HOMO and LUMO surfaces are highly delocalized. HOMO surface is mostly centered on the biphenyl rings, whereas the LUMO has extended to the third phenyl ring of the core. The oxygen of the carboxylic group attached directly with the biphenyl group is highly occupied compared to the other oxygen atoms of the molecule. The energy gap between highest occupied molecular orbit (HOMO) and lowest unoccupied molecular orbit (LUMO) is an important parameter to know about the stability of the compound. We calculated the energy gap between HOMO and LUMO from the simulated data. The gap was found to be 0.20388 a.u. This lower value suggests that 5F3R is a photochemically active molecule.

Using the simulated data we have calculated few important parameters of 5F3R, using standard calculations [12], which are listed in Table 1. The vibrational frequencies corresponding to the thermodynamic parameters were all found to be positive which implies the structure and the parameters to be thermally stable at the measuring temperature (298.15K). However to know the exact thermal stability of the parameters the optimization need to be done at various temperatures which is out of the scope of this work.

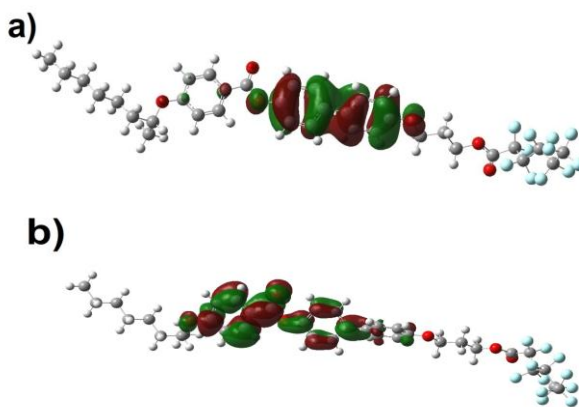


Fig. 5. a) HOMO and b) LUMO surfaces of 5F3R.

Table 1. A few optimized parameters of 5F3R. (simulated variable and thus the above parameters were calculated at temperature 298.15 K and at 1 atm pressure).

Parameters	Optimized values for 5F3R
Ionization potential	0.29871 au
Electronic affinity	0.09483 au
Electronegativity	0.19677 au
Global hardness	0.10194 au
Chemical potential	-0.19677 au
Chemical softness	9.809 au
$C_V$	177.44 cal/mol-K
Enthalpy	482.11 Kcal/mol
Entropy	311.36 cal/mol-K

### 3.2. Polarizing optical microscopy (POM)

As mentioned before, POM is an essential tool to determine the phase transition temperatures and phase type of liquid crystal compounds. LCs being optically active substances, in between cross polarizer they exhibit different optical patterns which arise due to topological defects of the compounds. As different phases of LCs have different types of topological defects so they have distinguishable optical textures. Thus temperature dependent texture observation can reveal the phase sequence of the compound. Two representative optical textures observed for 5F3R are shown in figure 6. The first one represents the optical texture of crystalline phase. In the second texture no major domain can be seen. However poorly developed traces of ‘broken fan’ texture can be observed here (marked by black box in the figure). Usually fan shaped textures are observed in SmA phase for the focal conic topological defect of this phase. In SmA phase the liquid crystal molecules are arranged in layers with the directors of molecules parallel to the layer normal. When SmC phase is generated by cooling from SmA phase, the phase structure doesn’t change much except an introduction of molecular tilt with respect to the layer normal. Thus in SmC phase broken fan shaped textures are observed [17]. However, in our compound the SmC phase was formed directly from isotropic phase skipping the formation of SmA. That is why the broken fan texture was developed poorly. Equidistant parallel lines can be observed throughout the texture. In chiral SmC\* phase, the molecules have permanent dipole moment and due to their mutual interaction the director rotates slowly from layer to layer forming a helical super structure. If the pitch of the helix is in order of several micrometer then equidistant lines, corresponding to the pitch can superimposed on the broken fan structure of SmC\* phase as we can see in our texture. Thus we can confirm that the compound has only one liquid crystal phase that is SmC\* phase. The transition temperature as measured by POM also matched with the same as reported earlier by other techniques [6,9].

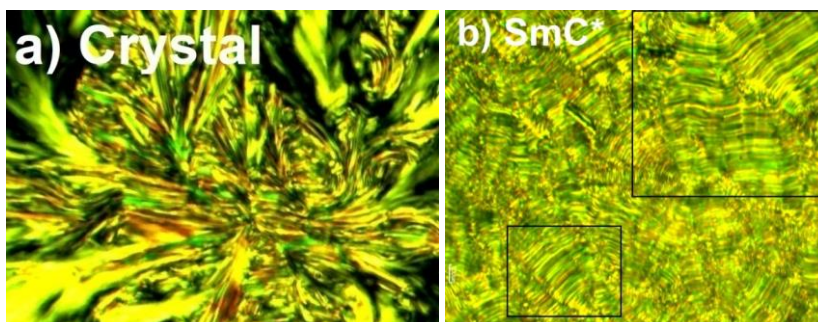


Fig. 6. Optical texture of 5F3R at a) Crystalline state b) SmC\* phase.

### 3.3. Optical tilt angle ( $\theta$ )

As mentioned before, in ferroelectric SmC\* phase the molecular long axis of the compound makes an angle with the smectics layer normal. According to Landau theory the tilt angle is the primary order parameter of phase transition in SmC\* phase [17-19]. Thus temperature variation of tilt angle in SmC\* phase can reveal important insights related to the phase transition of the specific compound. Apart from that the value of tilt angle is also important from application point of view. It had been established that for surface stabilized ferroelectric liquid crystal display (SSFLCD) the tilt angle of the FLC should ideally be  $22.5^\circ$  [20-22]. Thus it is important to know the value of the tilt angle of FLC to explore its suitability for display applications. Keeping that in mind the temperature variation of tilt angle of 5F3R was measured in SmC\* phase and the data near the phase transition was fitted with equation 1 [11], derived from mean field model.

$$\theta = \theta_0 \left(1 - \frac{T}{T_C}\right)^\beta [1]$$

Here  $T_C$  is the transition temperature from SmC\* to isotropic phase and  $\beta$  is the critical exponent of primary order parameter ( $\theta$ ). For ideal second order phase transition the value of  $\beta$  should be 0.5. The temperature variation of observed tilt angle of 5F3R is shown in Fig. 7.

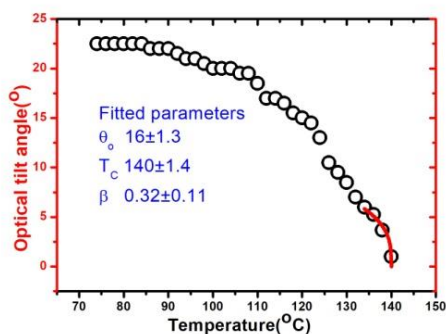


Fig. 6. Temperature variation of optical tilt angle of 5F3R.

The fitted value of transition temperature was found to match with POM study and previously published data [9]. The value of  $\beta$  deviates significantly from mean field value (0.5) of ideal 2<sup>nd</sup> order phase transition. This type of deviation was observed before for a compound 4F3R of same homologous series [23]. The maximum tilt angle of 5F3R was found to match exactly (22.5°) with the expected value for ideal SSFLCD, which can be proved to be useful from utilitarian perspective

#### 4. Conclusion

The molecular structure of a biphenyl benzoate cored liquid crystal compound was optimized using Hartree-Fock method with 3-21G basis. The molecule was found to have a strong dipole moment, which was expected for the fluorinated chain of the compound. The simulated IR spectrum revealed strongest absorptions for breathing of the phenyl rings in the core and C-F stretching in the fluorinated chain of the molecule. The low value of HOMO LUMO energy gap suggested that 5F3R can be a photochemically active compound. From the observation of optical texture the phase sequence and phase identification of the compound was reconfirmed. The chiral lines in the texture confirmed the chirality of SmC\* phase. The compound directly melted from SmC\* phase to isotropic phase which is quite rare for FLCs. From the fitted data of temperature variation of tilt angle of the compound it was found that the phase transition between SmC\* to isotropic phase deviated from ideal 2<sup>nd</sup> order phase transition which can be attributed to the absence of SmA\* phase in between SmC\* to isotropic phase. As the compound enters into liquid crystal phase at a temperature much higher than the room temperature thus it can't be directly used for the fabrication of LCDs. However, the facts that It showed a wide span of temperature for SmC\* phase and the highest value of the tilt angle (22.5°) matched exactly with the desired value for making SSFLCD, made 5F3R a promising compound to be used as a dope to fabricate a room temperature FLC mixture useful for display applications.

#### Acknowledgment

The author is grateful to R. Dabrowski, Military Institute of Technology, Warsaw, Poland for kindly supplying the liquid crystal sample. The author also likes to thank P. K. Mandal, Department of Physics, University of North Bengal, for kindly allowing the author to use his laboratory.

#### References

1. T. Sluckin, D. Dunmur, and H. Stegemeyer, Crystals That Flow: Classic Papers From the History of Liquid Crystals Liquid Crystals Book Series (Taylor & Francis, London, 2004). <https://doi.org/10.1201/9780203022658>
2. I. Mušević, R. Blinck, B. Zeks, The Physics of Ferroelectric and Antiferroelectric Liquid Crystals, 2<sup>nd</sup> Edition (World Scientific, New York, 1993) Vol. **267**(4).
3. R. B. Meyer, L. Liebert, L. Strzelecki, and P. Keller, J. Phys. Lett. **36**, 69 (1975).



- <https://doi.org/10.1051/jphyslet:0197500360306900>
4. A. K. Srivastava, V. G. Chigrinov, and H. S. Kwok, *J. Soc. Inf. Disp.* **23**, 253 (2015).  
<https://doi.org/10.1002/jsid.370>
  5. S. -H. Luo, Q. -F. Wang, Z. -Y. Wang, and P. Peng, *Res. Chem. Intermed.* **39**, 2513 (2013).  
<https://doi.org/10.1007/s11164-012-0777-5>
  6. D. Ziobro, R. Dąbrowski, M. Tykarska, W. Drzewiński, M. Filipowicz et al., *Liq. Cryst.* **39**, 1011 (2012).
  7. S. Ahmed, M. Rahman, A. R. Rabbi, K. Ahmed, S. M.S Islam et al., *J. Mol. Liq.* **224**, 265 (2016). <https://doi.org/10.1016/j.molliq.2016.10.002>
  8. P. Morawiak, W. Piecek, M. Żurowska, P. Perkowska, P. Perkowski, and Z. Perkowski, *Opto-Electron. Rev.* **17**, 40 (2009). <https://doi.org/10.2478/s11772-008-0044-x>
  9. D. Goswami, D. Sinha, and P. K. Mandal, *AIP Conf. Proc.* **1953**, ID 050012 (2018).
  10. D. Goswami, A. Debnath, P. K. Mandal, D. Węglowska, R. Dabrowski, and K. Czupryński, *Liq. Cryst.* **43**, 1548 (2016). <https://doi.org/10.1080/02678292.2016.1186755>
  11. S. T. Lagerwall, *Ferroelectric and Antiferroelectric Liquid Crystals* (Wiley-VCH, Newyork, 1999). <https://doi.org/10.1002/9783527613588>
  12. D. Sharma and S. N. Tiwari, *Emerg. Mater. Res.* **6**, 322 (2017).
  13. Gaussian 98, Revision A.11.4, M. J. Frisch, G. W. Trucks, H. B. Schlegel, G. E. Scuseria, M. A. Robb, J. R. Cheeseman, V. G. Zakrzewski, J. A. Montgomery, Jr., R. E. Stratmann, J. C. Burant, S. Dapprich, J. M. Millam, A. D. Daniels, K. N. Kudin, M. C. Strain, O. Farkas, J. Tomasi, V. Barone, M. Cossi, R. Cammi, B. Mennucci, C. Pomelli, C. Adamo, S. Clifford, J. Ochterski, G. A. Petersson, P. Y. Ayala, Q. Cui, K. Morokuma, N. Rega, P. Salvador, J. J. Dannenberg, D. K. Malick, A. D. Rabuck, K. Raghavachari, J. B. Foresman, J. Cioslowski, J. V. Ortiz, A. G. Baboul, B. B. Stefanov, G. Liu, A. Liashenko, P. Piskorz, I. Komaromi, R. Gomperts, R. L. Martin, D. J. Fox, T. Keith, M. A. Al-Laham, C. Y. Peng, A. Nanayakkara, M. Challacombe, P. M. W. Gill, B. Johnson, W. Chen, M. W. Wong, J. L. Andres, C. Gonzalez, M. Head-Gordon, E. S. Replogle, and J. A. Pople (Gaussian, Inc., Pittsburgh PA, 2002).
  14. D. Goswami, P. K. Mandal, and D. Węglowska, *Liq. Cryst.* **47**, 859 (2020).  
<https://doi.org/10.1080/02678292.2019.1686776>
  15. T. Theophanides, *Introduction to Infrared Spectroscopy*, in *Infrared Spectroscopy - Materials Science, Engineering and Technology* (InTech, 2012). <https://doi.org/10.5772/49106>
  16. K. Mounika, B. Anupama, J. Pragathi, and C. Gyanakumari, *J. Sci. Res.* **14**, 79 (2022).
  17. I. Dierking, *Textures of Liquid Crystal* (Wiley-VCH, Weinheim, 2003).  
<https://doi.org/10.1002/3527602054>
  18. P. Collings and M. Hird, *Introduction to Liquid Crystals Chemistry and Physics* (Taylor & Francis, London, 1997). <https://doi.org/10.4324/9780203211199>
  19. S. Chandrasekhar, *Liq. Cryst.* 2<sup>nd</sup> Edition (Cambridge University Press, New York, 1977).
  20. D. Węglowska, P. Perkowski, W. Piecek, M. Mrukiewicz, and R. Dąbrowski, *RSC Adv.* **5**, 81003 (2015). <https://doi.org/10.1039/C5RA14903G>
  21. A. Debnath, P. K. Mandal, D. Węglowska, and R. Dąbrowski, *RSC Adv.* **6**, 84369 (2016).  
<https://doi.org/10.1039/C6RA11238B>
  22. M. Hird, *Liq. Cryst.* **38**, 1467 (2011). <https://doi.org/10.1080/02678292.2011.625126>
  23. D. Goswami, D. Sinha, A. Debnath, P. K. Mandal, S. K. Gupta et al., *J. Mol. Liq.* **182**, 95 (2013). <https://doi.org/10.1016/j.molliq.2013.03.002>